# On the shape of a rapid hadron in QCD

B. Blok [a,*], L. Frankfurt [b], M. Strikman [c]

[a] *Department of Physics, Technion—Israel Institute of Technology, 32000 Haifa, Israel*
[b] *School of Physics and Astronomy, Raymond and Beverly Sackler Faculty of Exact Sciences, Tel Aviv University, 69978 Tel Aviv, Israel*
[c] *Physics Department, Penn State University, University Park, PA, USA*

A B S T R A C T

We visualize the fundamental property of pQCD: the smaller is the size of the colorless quark–gluon configuration, more rapid is the increase of its interaction with energy. Within the frame of the dipole model we use the $k_t$ factorization theorem to generalize the DGLAP approximation and/or leading $\ln(x_0/x)$ approximation and evaluate the interaction of the quark dipole with a target. In the limit of fixed $Q^2$ and $x \to 0$ we find the increase with energy of transverse momenta of quark (antiquark) within the $q\bar{q}$ pair produced by the strongly virtual photon. The average $p_t^2$ is evaluated analytically within the double logarithmic approximation. We demonstrate that the invariant mass$^2$ of the $q\bar{q}$ pair increases with the energy as $0.7 Q^2 (10^{-2}/x)^{0.4\alpha_s N_c/\pi}$, for transverse photons, and $\sim 0.7 Q^2 \exp 0.36[(\alpha_s N_c/\pi) \log(10^{-2}/x)]^{1/2}$ for longitudinal photons. We found similar pattern of the energy dependence of $M^2$ in the LO DGLAP approximation generalized to account for the $k_t$ factorization. We discuss the impact of the found phenomenon on the dependence of the coherence length on the collision energy and demonstrate that in the regime of complete absorption effective shape of the sufficiently energetic hadron (nucleus) has the biconcave form instead of the pancake. We explain that the different representations of chiral symmetry for the central and peripheral collisions would be characteristic property of hadron (nucleus) nucleus collisions at large energies. Some implications of the found phenomena for $pp$ collisions are discussed.

© 2009 Elsevier B.V. Open access under CC BY license.

## 1. Introduction

A dipole model developed in Ref. [1], cf. also [2–6] is the generalization of the of QCD evolution equations to the target rest frame description. It accounts for the effects of the $Q^2$ and $\ln(x_0/x)$ evolutions. It also provides the solution of the equations of QCD in the kinematics of fixed and not too small $x = Q^2/\nu$ but $Q^2 \to \infty$. The characteristic feature of this solution is the approximate Bjorken scaling for the structure functions of DIS, i.e. the two-dimensional conformal invariance for the moments of the structure functions. In this approximation as well as within the leading $\ln(x_0/x)$ approximation, the transverse momenta of quarks within the dipole produced by the local electroweak current are restricted by the virtuality of the external field:

$$\lambda_{\text{QCD}}^2 \leqslant p_t^2 \leqslant (Q^2)/4. \tag{1.1}$$

The aim of the present Letter is to demonstrate that the transverse momenta of (anti)quark of the $q\bar{q}$ pair produced by a local current

increase with energy and become larger than $Q^2$ at sufficiently large energies. Technically this effect follows from the more rapid increase with the energy of the pQCD interaction for smaller dipole size and $k_t$ factorization theorems.

It is worth noting that this effect is very different from the seemingly similar effect found in the leading $\alpha_s \log(x_0/x)$ BFKL approximation [7]: for the central rapidity kinematics $\log^2(p_t^2/p_{t0}^2) \propto \log(s/s_0)$. The latter is the property of the radiation within a ladder, of a diffusion in the space of the transverse momenta [7]. Indeed, it has been known for some time already that if we look at characteristic transverse momenta in a ring with a fixed number $N$ in BFKL ladder, than in the multiregge kinematics the transverse momenta do not depend on energy. This fact follows from the derivation of Lipatov diffusion equation, where $\log(p_t^2/p_{t0}^2) \propto N$— the number of the ring under study. The Lipatov diffusion arises since a number of rings $N$ in the ladder increases with the rapidity Y. An alternative proof that the transverse momenta do not rise in multiregge kinematics with a fixed number of rings has been given in Ref. [9]. On the other hand the property we are dealing here with is the value of the transverse momenta in the wave function of the projectile.

Within the double logarithmic approximation we evaluate analytically both the maximum in the distribution over the invariant

---

masses of the $q\bar{q}$ pair which contribute to the transverse and longitudinal total cross section of DIS, and the corresponding average transverse momenta squared.

Consider first the case of the longitudinal photons. Then the position of the maximum increases with energy as

$$M^2 = M_{1L}^2 (s/s_0)^{\alpha_s(N_c/\pi)/9}. \qquad (1.2)$$

Eq. (1.2) is derived in the approximation $Q^2 \ll M^2 \ll s$ which is self-consistent at sufficiently high energies. One can see from this expression that transverse momenta of quarks increase with the energy since $M^2 = p_t^2/z(1-z)$, and the configurations with $z = 1/2$ dominate at sufficiently high energies.

The dependence of the average quark transverse momenta on energy is calculated below numerically within the double logarithmic approximation and/or within the LO DGLAP and BFKL approximations. For certainty we define average transverse momentum of quark as corresponding to the median of integral for the total cross section. Within the double logarithmic approximation to the cross section initiated by longitudinal photon we obtain:

$$M_L^2 \sim 4 p_t^2 \sim 0.7 Q^2 \exp\big(0.36\big((\alpha_s N_c/\pi) \log(x_0/x)\big)^{0.55}\big). \qquad (1.3)$$

Here $x_0 \sim 0.01$. The analysis was done in the interval $s = 10^4$ to $s = 10^{11}$ GeV$^2$. Note that the derived rate of the increase with the energy of the characteristic scale does not depend on the external virtuality $Q^2$. However, $M_0^2$ depends on the normalisation point in $x_0$ and $Q_0^2$. It is worth emphasizing that since we are interested here in the proof of the rise of the transverse momenta in the current fragmentation region, we carry for the illustration, the calculations over a very wide spectrum of energies $s \sim 10^4$–$10^{11}$ GeV$^2$. The detailed calculations for the realistic energies have been carried in the LO approximation using the CTEQ5L gluon pdfs [10,11]. Qualitatively they produce similar results although depended on chosen extrapolation to small $x$. In particular the CTEQ6L parametrization leads to a significant suppression of the effects discussed in the Letter.

Similar results were obtained for the transverse photons. In this case we were able to carry out an analytical calculation for the invariant mass distribution maximum for the symmetric configurations and found that it rapidly increases with energy:

$$M_{1T}^2 \sim \big(M_0^2(s/s_0)\big)^{\alpha_s(N_c/\pi)/4}. \qquad (1.4)$$

The analytical results has been obtained in the kinematics: $Q^2 \ll M^2 \ll s$. It is well known however that in the case of the transverse photons a major role in a wide kinematical region is played by $q\bar{q}$ configurations where one of the partons carries most of the plus component of the photon momentum. With increase of the energy the role of asymmetric configurations is reduced since their contribution grows with energy more slowly. In order to take into account the asymmetric configurations we have made a numerical calculation of a transverse cross section in the interval $s = 10^4$–$10^{11}$ GeV$^2$, and obtained:

$$M_T^2 \sim 0.7 Q^2 (x_0/x)^{0.4\alpha_s N_c/\pi}, \qquad (1.5)$$

$x_0 \sim 0.01$.

Taking into account the increase of the transverse momenta of the dipole $p_t^2$ with energy within the framework of the dipole model and the $k_t$ factorization theorem lead to the generalization of the DGLAP [8] and BFKL [7] approximations which is done in the paper within the LO approximation.

The rapid increase of the characteristic transverse scales in the fragmentation region has been found first in Refs. [12–15], within the black disk (BD) regime. Our new result is the prediction of the increase with energy of the jet transverse momenta in the frag-

mentation region, in the kinematical domain where methods of pQCD are still applicable. This effect could be considered as a precursor of BD regime indicating the possibility of smooth matching between two regimes.

As the application of obtained results we obtain that in pQCD

$$\sigma_L(x, Q^2)/\sigma_T(x, Q^2) \propto (Q^2/4 p_t^2) \propto (Q^2/s)^\lambda, \qquad (1.6)$$

i.e. this ratio should decrease as the power of energy instead of being $O(\alpha_s)$.

The increase of the parton momenta in the DIS in the current fragmentation region leads to the change of many characteristics of high energy processes. In particular, the coherence length of the DIS processes increases with energy within pQCD as

$$\propto (1/2 m_N)\big(s/Q^2\big)^{1-\lambda}, \qquad (1.7)$$

i.e. slower than in the parton model ($1/2 m_N x$–the Ioffe length). This is the because the coherence length for a given process follows from uncertainty principle:

$$l_c = (s/2 m_N)/\big(M^2(s) + Q^2\big), \qquad (1.8)$$

where $M^2(s) \propto p_t^2(s)$ is the typical $M^2$ important in the wave function of photon in the target rest frame and $p_t$ is the transverse momentum of constituents in the wave function of photon. This result has the implication for the space structure of the wave packet describing a rapid hadron. In the classical multiperipheral picture of Gribov a hadron has a shape of a pancake of the longitudinal size $1/\mu$ (where $\mu$ is the soft scale) which does not depend on the incident energy [16]. On the contrary, we find the biconcave shape for the rapid hadron (nucleus) with the minimal longitudinal and transverse lengths for small impact parameter $b$ decreasing with increase of energy and being smaller for nuclei than for the nucleons.

The Letter is organized in the following way. In Section 2 using the technique first introduced in QED by Gribov [17], we rewrite the formulae of the dipole model for the inelastic cross section of DIS in the form of the spectral representation over invariant masses for both longitudinal and transverse photons. $k_t$ factorization [18,19] is explicitly fulfilled in this representation.

The analysis of these formulae predicts increase with energy of transverse quark momenta in the current fragmentation region. In Section 3 we use the double logarithmic approximation for the amplitude for the interaction of quark dipole with the target, to evaluate the increase with the energy of the quark transverse momenta in the current fragmentation region. In Section 4 we study the dependence of coherence length on the collision energy. In Section 5 we explain that in pQCD rapid hadrons and nuclei look like bi-concave lenses. Finally, in Section 6 we discuss the possible applications of our results to $pp$, $pA$ collisions at the LHC.

## 2. The target rest frame description

Within the LO approximation the QCD factorization theorem allows to calculate the total cross section of the longitudinally polarized strongly virtual photon scattering off a hadron target through the convolution of the virtual photon wave function calculated in the dipole approximation and the cross section of the dipole scattering off a hadron. In the target rest frame the cross section for the scattering of longitudinally polarized photon has the form [1,20,21]:

$$\sigma(\gamma_L^* + T \rightarrow X)$$
$$= \frac{e^2}{12\pi^2} \alpha_s \int d^2 p_t \, dz \langle \psi_{\gamma_L^*}(p_t, z) | \sigma(s, p_t^2) | \psi_{\gamma_L^*}(p_t, z) \rangle. \qquad (2.1)$$

Here $\sigma$ is the dipole cross section operator:

$$\sigma = (4\pi^2/3)\alpha_s(p_t^2)(-\Delta) \cdot xG(\tilde{x} = (M^2 + Q^2)/s, M^2), \qquad (2.2)$$

$\Delta$ is the two-dimensional Laplace operator in the space of the transverse momenta, and

$$M^2 = (p_t^2 + m_q^2)/z(1 - z), \qquad (2.3)$$

is the invariant mass squared of the dipole. In the coordinate representation $\sigma$ is just a multiplication, but not a differential operator. In the leading $\ln(x_0/x)$ approximation a similar equation arises where the cross section is expressed in terms of convolution of impact factor and unintegrated gluon density. In practice, both equations should give close results. Using an integration over parts over $p_t$ it is easy to rewrite Eq. (2.1) within the LO accuracy in the form where integrand will be explicitly positive:

$$\sigma(\gamma_L^* + T \to X)$$
$$= \frac{e^2}{12\pi^2} \int \alpha_s \, d^2 p_t \, dz \langle \nabla \psi_{\gamma_L^*}(p_t, z) | f(s, z, p_t^2) | \nabla \psi_{\gamma_L^*}(p_t, z) \rangle,$$
$$\qquad (2.4)$$

where

$$f = (4\pi^2/3)\alpha_s(p_t^2)xG(\tilde{x}, M^2). \qquad (2.5)$$

In the derivation we use boundary conditions that photon wave function is negligible at $p_t^2 \to \infty$ and that the contribution of small $p_t$ is the higher twist effect.

The cross section of the interaction of the longitudinal photon can be rewritten in the form of spectral representation by explicitly differentiating the photon wave function:

$$\sigma_L = 6\pi \frac{\pi \alpha_{\text{e.m.}} \sum e_q^2 F^2 Q^2}{12}$$
$$\times \int dM^2 \, \alpha_s(M^2) \frac{M^2}{(M^2 + Q^2)^4} \cdot g(\tilde{x}, M^2). \qquad (2.6)$$

Here $F^2 = 4/3$ for the colorless dipoles build of color triplet constituents, and $F^2 = 9/4$ for the gluonic dipoles.

The spectral representation of the electro-production amplitude over $M^2$ is a general property of a quantum field theory at large energies where the coherence length significantly exceeds the radius of the target T [22,23]. The pQCD guarantees additional general property: the smaller size of the configuration in the wave function of projectile photon leads to the smaller interaction with the target but this interaction more rapidly increases with the energy. In the NLO approximation the structure of formulae should be the same except the appearance of the additional $q\bar{q}g, \ldots$ components in the wave function of photon due to the necessity to take into account the QCD evolution of the photon wave function [20].

The similar derivation can be made for the scattering of the spatially small transverse photon. In this case the contribution of small $p_t$ region (Aligned Jet Model contribution) is comparable to the pQCD one. To suppress AJM contribution we restrict ourselves in the Letter by the region of large $p_t^2$ and sufficiently small $\tilde{x}$ where pQCD contribution dominates because of the rapid increase of the gluon distribution with the decrease of $x$.

The pQCD contribution into the total cross section initiated by the transverse photon has the form:

$$\sigma_T = 6\pi \frac{\pi \alpha_{\text{e.m.}} \sum e_q^2 F^2}{12}$$
$$\times \int_0^1 dz \int dM^2 \, \alpha_s(4M^2 z(1 - z))$$

$$\times \frac{z^2 + (1 - z)^2}{z(1 - z)} \frac{(M^4 + Q^4)}{(M^2 + Q^2)^4} \cdot g(\tilde{x}, 4M^2 z(1 - z)). \qquad (2.7)$$

Here while doing the actual calculations we introduced a cut-off in the space of transverse momenta $M^2 z(1 - z) \geqslant u$, $u \sim 0.3$ GeV$^2$.

## 3. The double logarithmic approximation

In this section we analyze the new properties of the pQCD regime within the double log approximation. The advantage of this approximation is that it will allow us to perform some of the calculations analytically. Other calculations will be made numerically but using the expressions that are known analytically.

In the double logarithmic approximation the structure functions are given by [24]

$$xG(x, Q^2) = \int dj/(2\pi i)(x/x_0)^{j-1}(Q^2/Q_0^2)^{\gamma(j)}, \qquad (3.1)$$

where the anomalous dimension is

$$\gamma(j) = \frac{\alpha_s N_c}{\pi(j - 1)}. $$

To simplify the calculation we assume, the initial condition for the evolution with $Q^2$:

$$g(x, Q_0^2) = \delta(x - 1). \qquad (3.2)$$

In the saddle point approximation one finds [24]:

$$xG(x, Q^2) = \frac{\log(Q^2/Q_0^2)^{1/4}}{\log(x_0/x)^{3/4}}$$
$$\times \exp\sqrt{4\alpha_s(Q_0^2)(N_c/\pi)\log(Q^2/Q_0^2)\log(x_0/x)}.$$
$$\qquad (3.3)$$

Structure function of a hadron is given by the convolution of this kernel with the nonperturbative structure function of a hadron in the normalization point $Q^2 = Q_0^2$. Note that $g$ is increasing with $Q^2$. This is the pQCD contribution where virtualities of exchanged gluons are large.

In the analysis of energy dependence of parton momenta it is legitimate to neglect the pre-exponential factor, since absolute value of $g$ as well as the pre-exponential factor weakly influence the transverse scale, and its evolution with energy:

$$xG(x, Q^2) = \exp\sqrt{4\alpha_s(Q_0^2)N_c/\pi \log(Q^2/Q_0^2)\log(x_0/x)}. \qquad (3.4)$$

### 3.1. Energy dependence of the quark transverse momenta for fragmentation processes initiated by longitudinal photon

We shall find analytically the scale of the transverse momenta in the limit where $s \gg M^2 \gg Q^2$. For certainty we restrict ourselves to the contribution of light quarks.

At large $Q^2$ the cross section for the scattering of the longitudinal photon is dominated by the contribution of the spatially small dipoles, so it is legitimate to neglect the quark masses. In this limit the cross section is proportional to

$$\sigma_L \propto Q^2 \int dM^2 \, n(M^2, s, Q^2), \qquad (3.5)$$

where the function $n(M^2, s, Q^2)$ is given by Eqs. (2.6), (2.7):

$$n(M^2, s, Q^2)$$
$$= \alpha_s(M^2/4) \frac{M^2}{(M^2 + Q^2)^4}$$

$$\times \exp \sqrt{4\alpha_s\big(Q_0^2\big)(N_c/\pi)\log\big(M^2/Q_0^2\big)\log\big(x_0 s/\big(M^2 + Q^2\big)\big)},$$
(3.6)

where $x_0 = Q^2/s_0$. Here we keep only large terms depending on $M^2$ (we ignore the $M^2$ independent normalization factor irrelevant for the calculations below).

Let us show that the maximum of $n(M^2, s, Q^2)$ increases with the energy. At very high energies $n$ is proportional to

$$n \sim \exp\big(\log \alpha_s\big(M^2/4\big) + \log\big(M^2/Q^2\big) - 4\log\big(\big(Q^2 + M^2\big)/Q^2\big)$$
$$+ \big[4\alpha_s(N_c/\pi)\big(\log(s/s_0)$$
$$- \log\big(\big(Q^2 + M^2\big)/Q_0^2\big)\big)\log\big(M^2/Q_0^2\big)\big]^{1/2}\big).$$
(3.7)

In the limit of fixed $Q^2$ but very large energies, $\log(s/s_0) \gg \log((Q^2 + M^2)/Q_0^2)$. Let us assume that for the maximum: $M^2 \gg Q^2$. We will find the maximum of the expression (3.7) under this assumption analytically, and then check that this assumption is indeed self-consistent. Indeed, differentiating the argument of the exponent over $\log(M^2/Q_0^2)$ we obtain the equation for the maximum:

$$1/\log\big(M^2/4Q_0^2\big) + 3$$
$$= (1/2)\big(1/\log\big(M^2/Q_0^2\big)$$
$$\times \sqrt{4\alpha_s\big(Q_0^2\big)(N_c/\pi)\log(s/s_0)/\log\big(M^2/Q_0^2\big)}\big).$$
(3.8)

Neglecting the small first term we find:

$$M^2 = M_0^2(s/s_0)^{\alpha_s(N_c/\pi)/9}.$$
(3.9)

Here $Q_0^2 \sim Q^2$ and $s_0 \sim Q^2$. We will refer to this extremum value of $M^2$ as $M_1^2$.

At the extremum $n \propto (\alpha_s(M_1^2/4)/M_1^6 \exp(N_c/\pi)(\alpha_s/3)\log(s/s_0))$. Therefore

$$\frac{d\sigma_L}{dM^2}\bigg|_{M^2=M_1^2} \approx \alpha_s\big(M_1^2/4\big)\big(Q^2/M_1^6\big)$$
$$\times \big(\exp(N_c/\pi)\big(\alpha_s\big(Q_0^2\big)/3\big)\log(s/s_0)\big).$$
(3.10)

However, the position of the maximum of the integrand is not sufficient to characterize the relevant transverse scales as a large range of $M^2$ is important in the integrand. In particular, calculation of second derivative shows that dispersion over $M^2 = M_1^2$ is large. The width of the distribution over $\log(M^2/M_0^2)$ is $\sqrt{2/3\log(M_1^2/M_0^2)}$.

Hence we need to determine $M^2$ range which gives most of the integrand support. For certainty, we define the range of $M^2 \leqslant M_t^2$ which provides a fixed, say, 50% fraction of the total perturbative cross section. Let us estimate how this scale increases with the energy in the double log approximation. First, let us consider the total cross section. The upper limit $u$ of integration over $M^2$ is determined by the kinematic condition through $t_{\min}$, giving that the allowed invariant masses $M^2 \ll s$.

For certainty we choose upper limit of integration as

$$M^2 \leqslant M_{\max}^2 = 0.2s,$$
(3.11)

from the cross section of diffraction although the result of numerical calculations is insensitive to the upper bound because essential $M^2$ are significantly smaller. In fact the integral for the cross section converges long before the upper limit of integration (3.11) is reached (see the discussion below).

Let us first calculate the median scale semi-analytically. Within the double logarithmic approximation, and assuming that the conditions $\log(s/s_0) \gg \log(Q^2 + M^2)/(Q^2 + M_0^2)$, is still valid for the relevant $M^2$, the integral for the cross section can be written similar as:

$$\sigma(u) = \big(Q^2/Q_0^4\big) \int_0^{\log(u/M_0^2)} d\log\big(M^2/Q_0^2\big)$$
$$\times \alpha_s\big(M^2/4\big)\exp\big(-2\ln\big(M^2/Q_0^2\big)$$
$$+ \sqrt{(4\alpha_s N_c/\pi)\log\big(M^2/Q_0^2\big)\log(s/s_0)}\big).$$
(3.12)

Here $u$ is the upper cut-off in the invariant masses. Introducing the new variable $t = \log(M^2/Q_0^2)$, we obtain:

$$\sigma(u) = \big(Q^2/M_0^4\big) \int_0^{\kappa(u)} dt\, \alpha_s\big(tM_0^2/4\big)$$
$$\times \exp\big(-2t + \sqrt{(4\alpha_s N_c/\pi)\log(s/s_0)t}\big),$$
(3.13)

where $\kappa(u) = \log(u/s_0)$. The integral for the total cross section is given by the equation similar to Eq. (3.13), with the upper integration limit being replaced by $\kappa(s) = \sqrt{\log(0.2s/s_0)}$. Note that the essential scale of integration is determined by exponent, and is very weakly influenced by the exact value of a upper cut-off. The integral (3.13) is actually the error function [25], which can be easily evaluated numerically. Requiring that it gives one half of the cross section we find

$$M_t^2 \sim Q_0^2(s/s_0)^{0.28\alpha_s N_c/\pi}.$$
(3.14)

Evidently, for sufficiently large $s$ our initial assumption $\log(M^2/Q_0^2) \gg \log(Q^2/Q_0^2)$ is fully self-consistent. This is because the decrease of $n$ with $M^2$ due to $1/M^6$ terms in the integrand of Eq. (2.6) is partially compensated by the rising exponential, giving a relatively slow decrease of $n$ to the right of the maximum of the integrand.

Note that the rate of the increase of $M_t^2$ with $s$ is much higher than for $M_1^2$ due to the slow decrease of the integrand with $M^2$. The cross section of jet production with $M^2$ at this interval also increases with the energy as

$$\frac{d\sigma}{dM^2}\bigg|_{M^2=M_1^2} \sim (s/s_0)^{0.24\alpha_s N_c/\pi}.$$
(3.15)

The analytical calculations supply the pattern for the behavior of the transverse momenta in double log approximation. In order to understand the dependence of the median scale on both the energy and $Q^2$ quantitatively in the double logarithmic approximation we made numerical calculation of the characteristic transverse momenta using the DGLAP double log structure function. We find that the increase rate of the transverse momenta indeed does not depend on the external virtuality $Q^2$. Considering the wide interval of energies and $s = 10^4$–$10^{11}$ GeV$^2$, and $20 < Q^2 < 200$ GeV$^2$ we obtain the approximate formulae:

$$M_t^2(x) \sim 0.7Q^2 \exp\big(0.17\big((4\alpha_s N_c/\pi)\log(x_0/x)\big)^{0.55}\big).$$
(3.16)

Here $x_0 = 0.01$.

The cross section of the jet production at this scale also increases with the energy as

$$\frac{d\sigma}{dM^2}\bigg|_{M^2=M_t^2} \sim \big(G\big(x, Q^2\big)/Q^6\big)\big(M_t^2(x)\big)$$
(3.17)

where $M_t^2(x)$ is given by Eq. (3.16).

The median transverse momenta $k_t^2 \sim M_t^2/4$, due to the dominance of symmetric configurations.

### 3.2. Transverse photon: The characteristic transverse scale in the photon fragmentation region

The main difference between the longitudinal and transverse structure functions in the DIS is the presence of the strongly asymmetrical in $z$ configurations due to the presence of the $(z(1-z))^{-1}$ factor in the spectral density. As a result there is a competition between two effects. One is a slower decrease of the spectral function with $M^2$ (by the factor $M^2/Q^2$), leading to the more rapid increase of the characteristic transverse momenta for the symmetric configurations. Another effect is the presence of the asymmetric ($z \to 0$) configurations which are characterized by the small transverse momenta $k_t^2$ for a given invariant mass $M^2$. For such configurations the rate of increase of the gluon structure function with energy is small. Let us first show that the transverse momenta increase rapidly for symmetric configurations. The spectral representation for the transverse photon for symmetric configurations is proportional to

$$
\begin{aligned}
& n\big(M^2, Q^2, s\big) \\
& \sim \frac{M^4 + Q^4}{(M^2 + Q^2)^4} \exp\Big[4\alpha_s(N_c/\pi)\big(\log(s/s_0) \\
& \quad - \log\big((Q^2 + M^2)/(Q_0^2)\big)\log\big(M^2/Q_0^2\big)\big)\Big]^{1/2}.
\end{aligned}
\tag{3.18}
$$

In the high energy limit, when $M_1^2 \gg Q^2$, we find for the dependence of the maximum of $n$ on energy:

$$
M_1^2 \sim Q_0^2 (s/s_0)^{\alpha_s(N_c/\pi)/4}.
\tag{3.19}
$$

This is twice as fast increase as for the case of longitudinal photon. $M_1^2$ increases with $s$ at high energies and thus the condition $M^2 \gg Q^2$ is perfectly self-consistent at very high energies.

In addition we can calculate the total cross section in the same approximation semi-analytically getting the error function and obtain the rate of increase $(s/s_0)^{0.14(4\alpha_s N_c/\pi)}$, which is twice that for the longitudinal case.

These two results are applicable to the symmetric configurations only. On the other hand, at least at achievable energies, the dominant contributions for transverse photon cross section are asymmetric, with z close to 0 or 1. In order to take these configurations into account we performed a numerical calculation using the gluon distribution function within the double log approximation. The result is that the characteristic median scale $M_t^2$ increases as

$$
M_0^2 \sim M^2\big(Q^2\big)(s/s_0)^{0.1(4\alpha_s N_c/\pi)}.
\tag{3.20}
$$

The value of the exponent is 0.12 for the beginning of the studied energy range $s \sim 10^4$–$10^{11}$ GeV$^2$, and decreases to 0.09 at the upper end (for typical $\alpha_s = 0.25$). Thus the rate of the increase with the energy is approximately the same as for longitudinal photons for not very high energies. For very high energies the symmetric configurations win over asymmetric ones, leading to the increase of the average transverse momentum squared which is twice as large as in the longitudinal case.

The precise determination of the scale $M_0^2(Q^2)$ is beyond the accuracy of this approximation. Effectively we obtain the dependence $M_t^2 \sim 0.7 Q^2 (x_0/x)^{0.1(4\alpha_s N_c/\pi)}$.

One can also estimate the rate of the increase of the jet production cross section:

$$
d\sigma_T/dM_{M_t^2}^2 \sim \big(xG\big(x, Q^2\big)/Q^4\big)(1/3)\big(1 + 0.5(x_0/x)^{0.24}\big).
\tag{3.21}
$$

We found a rapid increase of the jets multiplicity with energy. Thus the rate of the increase with energy of the transverse momenta of quarks in the current fragmentation region for transversely polarized photon is significantly more rapid. Consequently we find that $\sigma_L/\sigma_T \approx \alpha_s Q^2/M^2$ being numerically small should slowly decrease with energy at sufficiently high energies.

We conclude that it is possible to show analytically that for very high (asymptotic) energies the relevant invariant masses extend well beyond $Q^2$ and increase with the energy.

The direct numerical calculation of the $M_t^2$ scale shows that the rate of increase is independent of external virtuality. Note that due to the significant contribution of the asymmetric configurations the median transverse momenta is much smaller than $M_t^2/4$. The simple numerical calculations using $k_t^2 = M^2 z(1-z)$, shows that the average transverse momenta (including nonsymmetric configurations) rapidly increases like $a(Q^2)/(x/0.01)^{0.12}$, with the exponent once again is independent of external virtuality, and $a(Q^2) \sim 0.6$ GeV$^2 + 0.02 Q^2$, i.e. $k_t^2$ is much smaller that $M^2/4$, especially for small virtualities.

### 3.3. The running coupling constant

In the previous subsections we considered the case of the double logarithmic approximation with fixed coupling constant. Allowing for the running coupling constant in the saddle point approximation leads qualitatively to the same results. Indeed, the structure function is given by [24]

$$
xG\big(x, Q^2\big) = \exp\sqrt{(4N_c/\pi b) \log\frac{\log(Q^2/\lambda^2)}{\log(Q_0^2/\Lambda^2)} \log(x_0/x)}
\tag{3.22}
$$

(up to slow pre exponential factor that is irrelevant for the discussion below). Here $b = N_c - 2N_f/3$ is the coefficient in the $\beta$ function depended on the number of flavors. Eq. (3.22) allows to find the dependence of the maximum of the integrand for the cross section over $M^2$ as a function of energy. We obtain for the maximum of cross section initiated by longitudinal photons (for symmetric configurations initiated by transverse photon) with the logarithmic accuracy:

$$
M^2 = Q^2 \exp\frac{1}{3}\sqrt{\frac{N_c}{\pi b} \log(s/s_0)}.
\tag{3.23}
$$

The maximum shifts to the right with the energy increase. The same analysis can be made for the symmetric configurations for the processes initiated by transverse photons.

Numerical analysis shows that the median of transverse momenta continues to rise both for transverse and longitudinal photons.

### 3.4. The leading logarithmic approximation

The above results were obtained in the double logarithmic approximation. It is also possible to carry out the numerical calculation in LO approximation using the CTEQ5L gluon distribution functions [10]. In this approximation $M_t^2 \sim 0.7 Q^2 (x_0/x)^{\lambda}$, where $x_0 \sim 10^{-2}$, and $\lambda \sim 0.06$ for longitudinal and $\lambda \sim 0.1$ for transverse photons. The rise of momenta is not negligible: for energy increase from $10^4$ to $10^7$ GeV$^2$ the scale increases by a factor $\sim 1.5$. The use of CTEQ6L will somewhat decrease the considered effects.

## 4. The coherence length in DIS

It was understood already in the sixties by Ioffe [27] that the essential longitudinal distances in DIS = coherence length are $l_c \sim 1/2m_N x_B$ i.e. $l_c$ increases linearly with collision energies within the parton model approximation. This important behavior follows naturally from the multiperipheral Gribov picture for hadron–hadron collisions [16] where the longitudinal size of the hadron is determined by the $ee$ parton cloud and energy independent $L_z \sim 1/\mu$. Here $\mu \sim 0.3$–$0.4$ GeV/$c$ is the scale of soft QCD interactions.

Numerical analysis of coordinate space representation of target structure functions in the target rest frame (similar to that in [26]) found that coherence length significantly less rapidly increases with energy in QCD as compared to the parton model as result of $Q^2$ evolution [33,34]:

$$l_c = (1/2m_N x)(s_0/s)^\lambda. \tag{4.1}$$

Here $\lambda$ coresponds to the rate of increase of transverse momenta for relevant gluon configurations in the nucleon. This pattern of the energy dependence of the coherence length follows from the different dependence on energy of life-time of different configurations in the wave function of the rapid dipole. In the previous sections we found that the effective transverse scale of dominant processes in DIS increases with energy which further slowed down increase with energy of coherence length as compared to the above formulae.

On the other hand more rapid increase with energy of cross sections of hard processes than soft ones and a slower than $(1/2m_N x)$ rate of the increase of the coherent length with energy for hard processes should have significant impact on the space–time evolution of hadron collisions. In the next section we evaluate change of the shape of rapid hadron (nucleus) because of slowing down of increase with energy of coherence length in the hard processes.

## 5. The shape of energetic nucleon, nucleus

Increase with the energy of the parton momenta in the wave function of virtual photon and slowing down of increase with energy of coherence length are valid beyond the region of applicability of pQCD, in the regime of complete absorption—the black disc regime (BDR) [12]. The focus of our discussion in this section is the impact of this property of QCD combined with the rapid increase with energy of hard interactions found in QCD and in deep inelastic processes on the shape of wave function (w.f.) of sufficiently energetic hadron (nucleus). This is vast subject so we restrict ourselves by the analysis of the transverse structure of sufficiently energetic hadrons and nuclei. Our interest is in the kinematics where BDR is achieved for hard interactions since in this kinematics calculations are especially simple.

Let us consider the longitudinal distribution of the partons in an energetic hadron. As it was already mentioned in the previous section, in the parton model the longitudinal spread of the gluonic cloud is $L_z \sim 1/\mu$ for the wee partons (where $\mu$ is the soft scale) and it is much larger than for harder partons, with $L_z \sim 1/xP_h$ for partons carrying a finite $x$ fraction of the hadron momentum [16]. The picture is changed qualitatively in the limit of very high energies when dipole–hadron interactions at central impact parameters reach BD regime for $k_t \gg \mu$. In this case the smallest possible characteristic momenta of partons interacting with a quark of dipole are of the order $k_t(\mathrm{BDR})$ which is a function of both initial energy and transverse coordinate, impact parameter $b$ of the hadron. Correspondingly, the longitudinal size of this hadron is $\sim 1/k_t(\mathrm{BDR}) \ll 1/\mu$. Note here that we are discussing longitudinal distribution for typical partons. There is always a tail to the momenta much smaller than typical one all the way down to $k_t \sim \mu$ which corresponds to the partons with much larger longitudinal size (a pancake of soft gluons corresponding to the Gribov's picture). However at large energies at the proximity of the BDR the contribution of the gluons with $k_t < k_{tb}$ is strongly suppressed [28]. In the BDR this tail is suppressed by a factor $k_t^2/k_t(\mathrm{BDR})^2$ in addition to the phase factor [12]. In the color glass condensate model the suppression is exponential [29].

Since the gluon parton density decreases with the increase of $b$ the longitudinal size of the hadron is larger for large $b$, so a hadron

has a shape of biconcave lens, see Figs. 1, 2. It is of interest also that for the zero impact parameter the longitudinal size of a rapid nucleus is smaller than of a nucleon. This property follows from the fact that at central impact parameters $k_t(\mathrm{BDR}\,A) \gg k_t(\mathrm{BDR}\,N)$.

In the numerical calculation we took

$$|l_z| = 1/k_t(\mathrm{BDR}), \tag{5.1}$$

neglecting all factors of the order of one (typically in the Fourier transform one finds $\langle z \rangle \sim \frac{\pi}{\langle p_z \rangle}$). We calculated $k_t(\mathrm{BDR})$ for fixed external virtuality $Q^2 \sim 40$ GeV$^2$. Our results are not sensitive to the value of $Q^2$, as the value of $Q^2$ only enters in the combination $x' = (Q^2 + M^2)/s$, and the $k_t^2$ we found were comparable or larger than $Q^2/4$. Indeed, the direct calculation shows that for small $b$ the change of $1/k_t$ between external virtualities of 60 and 5 GeV$^2$ is less than 5%. Such weak dependence continues almost to the boundary of Fig. 1 where $k_t \sim 1$ GeV. Near the boundary the uncertainty increase to $\sim 25\%$, meaning that for large b (beyond those presented at Fig. 1) the nucleon once again becomes a pancake and there is a smooth transition between two pictures (biconcave lens and pancake). We want to emphasize here that the discussed above weak dependence of $k_t(\mathrm{BDR})$ on the resolution scale indicates that the shape of the wave function for small $x$ is almost insensitive to the scale of the probe.

We present our calculations of the typical transverse quark distributions within the energetic nucleon in Fig. 1. It is drastically different from the naive picture of a fast moving nucleon as a flat narrow disk with small constant thickness. (Similar plot for the gluon distribution is even more narrow.) Note also that for the discussed small $x$ range $k_t \geqslant 1$ GeV/$c$ for $b \leqslant 1$ fm. Since the spontaneous chiral symmetry breaking corresponds to quark virtuality $\mu^2 \leqslant 1$ GeV$^2$, probably $\sim 0.7$ GeV$^2$ [32], corresponding to $k_t \sim \sqrt{\frac{2}{3}\mu^2} \sim 0.7$ GeV/$c$ the chiral symmetry should be restored for a large range of central impact parameters $b$ in the proton wave function for sufficiently small $x$.

Let us discuss the case of the DIS off a nucleus.

First, we consider the case of external virtualities of the order of several GeV. In this case the shadowing effects to the large extent cancel the factor $A^{1/3}$ in the gluon density of a nucleus for a central impact parameters, $b$ [30], and the gluon density in the nuclei is comparable to that in a single nucleon for $b \sim 0$. Consequently over the large range of the impact parameters the hadron longitudinal size is approximately the same for the scattering off nuclear and nucleon targets.

However for very small $x$ $4k_t^2(\mathrm{BDR}) \geqslant 40$ GeV$^2$. This is a self consistent value as indeed for such $Q^2$ the leading twist shadowing is small.

Accordingly we calculated the shape of the nucleus for the external virtuality $Q^2 \geqslant 40$ GeV$^2$. We should emphasize here that taking a smaller virtuality would not significantly change our result for $k_t(\mathrm{BDR})$ (at the same time LT nuclear shadowing reduces a low momentum tail of the $k_t$ distribution).

In the discussed limit of the small leading twist shadowing, the corresponding gluon density unintegrated over $b$ is given by a product of a nucleon gluon density and the nuclear profile function:

$$T(b) = \int dz\, \rho(b, z), \tag{5.2}$$

where the nuclear three-dimensional density is normalized to $A$. We use standard Fermi step parametrization [31]

$$\rho(r) = C(A)\frac{A}{1 + \exp((r - R_A)/a)},$$
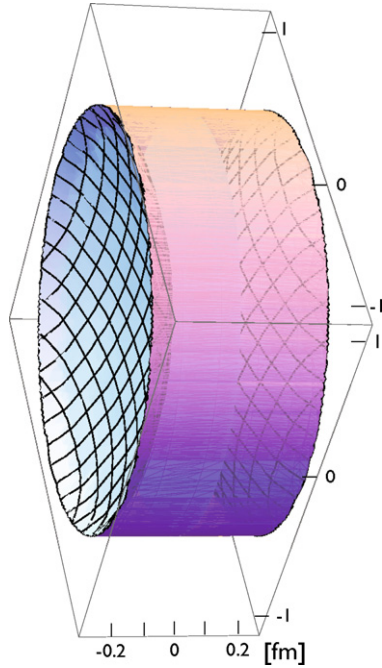$$R_A = 1.1A^{1/3} \text{ fm}, \ a = 0.56 \text{ fm}. \tag{5.3}$$

**Fig. 1.** 3D image of the fast nucleon at $s = 10^7$ GeV$^2$ and $Q^2 = 40$ GeV$^2$.

Here $r = \sqrt{z^2 + b^2}$, and $A$ is the atomic number. $C(A)$ is a normalization factor, that can be calculated numerically from the condition $\int d^3r\,\rho(r) = A$. At the zero impact parameter $T(b) \approx 0.5A^{1/3}$ for large $A$.

The dependence of the thickness of energetic nucleus as a function of the transverse size is described in Fig. 2 for the typical high energy $s = 10^7$ GeV$^2$, $Q^2 = 40$ GeV$^2$. We see that the nuclei also has a form of a biconcave lens instead of a flat disk. The dependence on the external virtuality for the nuclei is qualitatively very similar to the case of the nucleon. For small $b$ the dependence is very weak (of order 5%) and increases only close to the boundary of the biconcave lens region where it is of order 20% (and $k_t \sim 1$ GeV). For larger b the nucleus wave function smoothly returns to the pancake picture.

Note that this picture is very counterintuitive: the thickness of a nucleus is smaller than of a nucleon in spite of $\sim A^{1/3}$ nucleons at the same impact parameter. The resolution of the paradox in the BD regime is quite simple: the soft fields of individual nucleons destructively interfere cancelling each other. Besides for a given impact parameter $b$, the longitudinal size of a heavy nucleus $1/k_t^{(A)}$(BDR) $< 1/k_t^{(p)}$(BDR) since the gluon distribution function in the nuclei $G_A(x, b) > G_N(x, b)$. So a naive classical picture of a system build of the constituents being larger than each of the constituents is grossly violated. The higher density of partons leads to the restoration of the chiral symmetry in a broad $b$ range and much larger $x$ range than in the nucleon case.

## 6. Experimental consequences

The current calculations of cross sections of hard processes at the LHC are based on the use of the DGLAP parton distributions and the application of the factorization theorem. Our results imply that the further analysis is needed to define the kinematic regions where one can use DGLAP distributions. We showed in the Letter that for DIS at high energies there are kinematic regions where one is forced to use a $k_t$ factorization and the dipole model instead of the direct use of DGLAP. A similar analysis must be made for the $pp$ collisions at LHC. The expected effect is the increase with
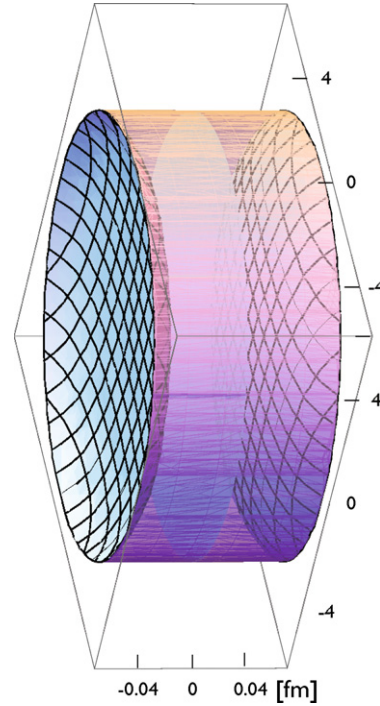


**Fig. 2.** 3D image of the fast heavy nucleus (gold) at $s = 10^7$ GeV$^2$ and $Q^2 = 40$ GeV$^2$.

energy of the probability of the small dipoles in the wave function of proton.[1] Quantitative analysis of this problem will be presented elsewhere.

The hard processes initiated by the real photon can be directly observed in the ultrapheripheral collisions [35]. The processes where a real photon scatters on a target, and creates two jets with an invariant mass $M^2$, can be analyzed in the dipole model by formally putting $Q^2 = 0$, while $M^2$ is an invariant mass of the jets. In this case with a good accuracy the spectral density discussed above will give the spectrum of jets in the fragmentation region. Our results show that the jet distribution over the transverse momenta will be broad with the maximum moving towards larger transverse momenta with increase of the energy and centrality of the $\gamma A$ collision.

Theoretical analysis of wave function of sufficiently energetic hadron (nucleus) found in the Letter that different phases of chiral symmetry should dominate at different impact parameters. This property leads to two phase structure of hadron–nucleus, nucleus–nucleus collisions. Central and peripheral collisions correspond to different representations of chiral symmetry-resemblance to second order phase transition.

Finally, our results can be checked directly, if and when the LHeC facility will be built at CERN.

## References

[1] S.J. Brodsky, L. Frankfurt, J.F. Gunion, A.H. Mueller, M. Strikman, Phys. Rev. D 50 (1994) 3134.

---

[1] We are indebted to S. Brodsky for emphasizing this point.

[2] H. Abramowicz, L. Frankfurt, M. Strikman, Surv. High Energy Phys. 11 (1997) 51.
[3] L. Frankfurt, G.A. Miller, M. Strikman, Annu. Rev. Nucl. Part. Sci. 44 (1994) 501.
[4] B. Blaettel, G. Baym, L. Frankfurt, M. Strikman, Phys. Rev. Lett. 70 (1993) 896.
[5] A.H. Mueller, Nucl. Phys. B 415 (1994) 373.
[6] J.C. Collins, L. Frankfurt, M. Strikman, Phys. Rev. D 56 (1997) 2982.
[7] E. Kuraev, V. Fadin, L. Lipatov, Sov. Phys. JETP 44 (1976) 443;
E. Kuraev, V. Fadin, L. Lipatov, Sov. Phys. JETP 45 (1977) 199;
I. Balitsky, L. Lipatov, Sov. J. Nucl. Phys. 28 (1978) 822.
[8] G. Altarelli, G. Parisi, Nucl. Phys. B 126 (1977) 298;
V.N. Gribov, L.N. Lipatov, Sov. J. Nucl. Phys. 15 (1972) 438;
V.N. Gribov, L.N. Lipatov, Sov. J. Nucl. Phys. 15 (1972) 672;
Yu.L. Dokshitser, Sov. Phys. JETP 46 (1977) 641.
[9] L. Frankfurt, V. Sherman, Phys. Lett. B 61 (1976) 70.
[10] B. Blok, L. Frankfurt, M. Strikman, arXiv:0904.1450.
[11] B. Blok, L. Frankfurt, M. Strikman, arXiv:0808.2006 [hep-ph], talk at small x conference, Columpari, Crete, July 2008.
[12] V. Guzey, L. Frankfurt, M. Strikman, M. McDermott, Eur. J. Phys. C 16 (2000) 641.
[13] L. Frankfurt, M. Strikman, C. Weiss, Annu. Rev. Nucl. Part. Sci. 55 (2005) 403.
[14] T.C. Rogers, A.M. Stasto, M.I. Strikman, arXiv:0801.0303 [hep-ph].
[15] T.C. Rogers, M.I. Strikman, J. Phys. G 32 (2006) 2041.
[16] V.N. Gribov, hep-ph/0006158.
[17] V.N. Gribov, The Theory of Complex Angular Momenta: Gribov Lectures on Theoretical Physics, Cambridge University Press, Cambridge, UK, 2003.
[18] S. Catani, M. Ciafaloni, F. Hauptmann, Nucl. Phys. B 366 (1991) 135.
[19] J. Collins, K. Ellis, Nucl. Phys. B 360 (1991) 3.
[20] L. Frankfurt, M. Strikman, Phys. Rep. 160 (1988) 235.
[21] L. Frankfurt, A. Radyushkin, M. Strikman, Phys. Rev. D 55 (1997) 98.
[22] V.N. Gribov, Sov. Phys. JETP 30 (1970) 709.
[23] T.H. Bauer, R.D. Spital, D.R. Yennie, F.M. Pipkin, Rev. Mod. Phys. 50 (1978) 261;
T.H. Bauer, R.D. Spital, D.R. Yennie, F.M. Pipkin, Rev. Mod. Phys. 51 (1979) 407, Erratum.
[24] Yu. Dokshitzer, D. Diakonov, S. Troyan, Phys. Rep. 58 (1980) 269.
[25] M. Abramowitz, I. Stegun, Handbook of Special Functions, Dover Publications, New York, 1964.
[26] L.B. Ioffe, V. Gribov, I. Pomeranchuk, Sov. J. Nucl. Phys. 2 (1966) 549.
[27] B.L. Ioffe, Phys. Lett. B 30 (1969) 123.
[28] A.H. Mueller, Nucl. Phys. A 702 (2003) 65.
[29] A. Dumitru, J. Jalilian-Marian, Phys. Rev. Lett. 89 (2002) 022301, arXiv:hep-ph/0204028.
[30] L. Frankfurt, V. Guzey, M. Strikman, Phys. Rev. D 71 (2005) 054001.
[31] A. Bohr, B.R. Mottelson, Nuclear Structure, vol. 1, W.A. Benjamin, New York, 1969.
[32] D. Diakonov, V.Y. Petrov, Nucl. Phys. B 272 (1986) 457.
[33] Y. Kovchegov, M. Strikman, Phys. Lett. B 516 (2001) 314.
[34] B. Blok, L. Frankfurt, Phys. Lett. B 630 (2005) 49.
[35] L. Frankfurt, M. Strikman, Phys. Rep. 455 (2008) 105.